Beta-spectra for the Radionuclides in Medicine

Chul-Young Yi*[1], Kyung-Hwa Kim[1], Kyung-Bae Park[1], Hyon-Soo Han[1], Jae-Shik Jun[2], Ha-Seok Chai[2]

[1]*Korea Atomic Energy Research Institute, HANARO Center, P.O.Box 105, Taejon 305-600 and* [2]*Chungnam National University, Department of Physics, Taejon 305-764*

Beta-particle energy distributions of the radionuclides in medicine are calculated for the medical physics applications. The radial component solutions of Dirac wave equations are evaluated for a point-nucleus unscreened Coulomb potential. The WKB method is employed to correct the screening due to the orbital-electron cloud. Fierz interference terms are ignored. The radionuclides considered are ^{32}P, ^{90}Y, ^{131}I, ^{166}Ho, ^{192}Ir, ^{198}Au, ^{153}Sm, ^{169}Er and ^{188}Re. A total of 9 beta-spectra for the radionuclides, currently in domestic use or potential use in the near future, are calculated with enough accuracy and presented in graphs and tables.

INTRODUCTION

Knowledge on the shapes of beta-ray spectra is a matter of great concern in dosimetry and other radiation physics applications. It is well known that differences in spectral shapes are primarily responsible for variations in the shapes of depth-dose distributions obtained from different beta emitters having nearly the same end-point energies[1].

In the passage through matter, monoenergetic electrons and positrons experience numerous interactions. The predominant interactions of electrons with atoms are through Coulombic collisions. These can be separated into those that are inelastic, resulting in energy loss, production of secondary radiation and change of the incident direction, and those that are elastic, resulting only in a change of the incident direction. Information on Baba or Møller cross-section, annihilation cross-section and bremsstrahlung cross-section in connection with photon interaction cross-sections with matter, angular distribution for multiple or single elastic scattering, energy loss straggling distribution, and radiative and collision stopping powers is generally required to formulate an electron transport equation and evaluate the resultant energy deposition. All the physical quantities above are energy-dependent. Accordingly, beta-dose is obtained from that of monoenergetic electrons weighted by the energy distribution of beta-particles.

Extensive tabulations of the Fermi function and the related quantities were carried out by Fano[2], Dismuke *et al.*[3], Rose *et al.*[4], and Behrens and Jänecke[5]. Starting from as early as 1940s, compilations on beta-ray spectra and their average energies were presented by a number of authors[6-9]. However, most of the previous compilations on beta-ray spectra were based on the evaluation of the approximate expression for the Fermi function.

We calculate the energy distribution of beta

particles for several radionuclides frequently introduced in medical applications and for those in the development stage at KAERI (Korea Atomic E nergy Research Institute) and other domestic institutes equiped with particle accelerators. The radial components of the continuous spectrum solutions of the Dirac wave equation for a point-nucleus in an unscreened central Coulomb field are evaluated at the nuclear radius. Corrections for the potential shift due to screening and finite size effect of the nucleus is carried out thereafter. The beta-spectra for an allowed and first forbidden unique transitions can be obtained from the bilinear combinations of the continuous spectrum solutions.

To the authors' knowledge, ^{32}P, ^{90}Y, ^{131}I, ^{166}Ho, ^{192}Ir and ^{198}Au are currently in use in hospitals and medical institutions. Development of the radionuclides such as ^{153}Sm, ^{169}Er and ^{188}Re are in progress for commercial use in medicine. The beta-spectra of the radionuclides above are given in graphs and tables in the present study.

METHOD

The energy distribution of beta-particles has been studied recently by the authors[10]. Here, we review it briefly. The number of beta-particles $N(W)$ with energies $W \sim W + dW$ emitted per unit time in a single transition, and in the system of units such that $\hbar = m = c = 1$, is given by

$$N(W)dW = \frac{g^2}{2\pi^3} S_n(Z, W)\, p\, W (W_0 - W)^2 dW \tag{1}$$

where S_n is the shape factor and the subscript, n designates an "allowed" or "n-th forbidden transition", W_0 is the maximum energy available to beta-particles in the transition, p is the momentum of beta-particles and Z is the atomic number of the residual nucleus. For an n-th forbidden transition, the nuclear parities are such that $(\pi_i)\cdot(\pi_f) = (-1)^n$ and its nuclear spin change is either $\Delta J = n$ or $\Delta J = n+1$, except that the first forbidden transition includes $\Delta J = 0$. Since all the radionuclides considered are negatron emitters, evaluations are restricted to negatron decays in the present study.

Due to Gove and Martin[11], and Warburton *et al.*[12], the shape factors for the allowed and the unique forbidden transitions can be written as follows:

$$S_n(Z, W) = \frac{(2n+1)(2n+1)!}{[(2n+1)!!]^2} C_A^2 \langle G_n \rangle^2 \times \sum_{k=1}^{n+1} \frac{\lambda_k(Z, W)\, p^{2(k-1)} (W_0 - W)^{2(n-k+1)}}{(2k-1)![2(n-k+1)+1]!} + C_V^2 \langle 1 \rangle^2 \lambda_1(Z, W)\, \delta_{n,0} \tag{2}$$

where $\langle G_n \rangle^2 = \frac{4\pi}{(2n+1)} \langle R^n \sigma \cdot T^n_{n+1} \rangle^2$, $\lambda_k(Z, W) = \frac{g_{-k}^2 + f_k^2}{2p^2} \left[\frac{(2k-1)!!}{(pR)^{k-1}} \right]^2$, R is the radius of a nucleus, $\delta_{n,0}$ is the usual Dirac-delta notation, and C_A and C_V are the dimensionless coupling constants for the axial-vector and vector interactions, respectively. Since the average nuclear density is found to be independent of the total number of nucleons, it is usually assumed that $R = r_0 A^{1/3}$, where r_0 is found empirically. The reduced matrix element $\langle \sigma \cdot T^n_{n+1} \rangle^2$ and $\langle 1 \rangle^2$ are kindly explained in the text[13]. The radial components f_x and g_x are the solutions of the coupled set of Dirac wave equations. No analytical solution exists, but those for a point-nucleus unscreened Coulomb potential. They are

$$\begin{pmatrix} f_x \\ g_x \end{pmatrix} = \frac{(1 \mp W)^{1/2}(2pR)^{\gamma_x} e^{\pi y/2} |\Gamma(\gamma_x + iy)|}{2RW^{1/2}\Gamma(2\gamma_x + 1)}$$
$$\times [e^{-ipr+i\eta}(\gamma_x + iy).$$
$$\times F(\gamma_x + 1 + iy,\ 2\gamma_x + 1\ ;\ 2ipR) \mp c.c.\ ] \quad (3)$$

where $\gamma_x = (x^2 - \alpha^2 Z^2)^{1/2}$, $y = \pm \alpha ZW/p$, $e^{2i\eta} = \frac{-(x - iy/W)}{\gamma_x + iy}$, F is the confluent hypergeometric function, α is fine structure constant and $c.c$ means the complex conjugate of $e^{-ipr+i\eta}(\gamma_x + iy) \times F$. The screening correction is determined by using the WKB procedure[14]. The main uncertainty in the screening correction arises from the uncertainty of the potential shift near the nucleus caused by the screening. In the present study, we have formulated an expression which fits the tabulated values of Matese and Johnson[15]. Futhermore, the correction for the finite nuclear size is required since Equation (3) is evaluated for a point nucleus. We have used a simple approximate expression for the correction to λ_k which is carefully given in the literature of Gove and Martin[11]. On the basis of the experimental evidence[16] concerning the magnitude of correction for the Fierz interference, we ignored it.

Transition rates, end-point energies, spins and parities[17] for the radionuclides considered are shown in Table 1. Spectra with transition rates less than 0.1% are ignored. The experimental shape factors compiled by Behrens and Szybisz[18] are used in preference to Equation (2).

It is presently not possible to calculate the shapes of non-unique forbidden spectra since the unknown nuclear matrix elements are combined with the energy-dependent terms and in general, they can not be factored out[19-22]. For the first forbidden non-unique spectrum, Wapstra[19], Bühring[20] and Daniel[22] suggested the shape factors in the form of $[1 + c_1(W_0 - W)]^2$, $1 + c_2/W$ and $1 + c_3 W + c_4/W + c_5 W^2$, respectively, where c_i can be determined experimentally. As a first approximation, we assume that the first forbidden non-unique spectrum treated is in the allowed shape.

The composite spectrum is calculated from the relation:

$$N(W) = \sum_{i=1}^{M} f_i N_i(W) \quad (4)$$

where M is the number of beta spectra emitted by the isotope under consideration, f_i is the frequency of emission for the i-th spectrum and $N_i(W)$ is the number of beta-particles of total energy W in the i-th spectrum.

RESULT AND DISCUSSION

For the maximum end-point energy range 50 keV to 5 MeV, $Z = 10$ to 90, and $A = 20$ to 230, we compared our $Log\text{-}f_n^{\pm}$ values calculated for the allowed and first forbidden unique transitions with those given by Gove and Martin[11]. In most cases, the agreement is better than 0.1%. But, the agreement becomes worse for low-energy, high-Z negatron emitters for which $Log\text{-}f_n^{\pm}$ values are susceptible to the individual WKB-treatment of the negatron energy in the vicinity of the screening potential, where p and W turn into the unphysical. Even in such cases, the agreement remains within a few tenths of a percent and never exceeds 1.1%.

The spectra of the selected beta-emitters familiar to the eye of radiation physicist are shown in Figure 1. The calculated average energies shown in the Figure agree, on the whole, with those in other literatures[6-9] within a few percent. It should be mentioned that most of the previous studies on the shapes of beta spectra and the average energies were calculated using the approximate expressions of Fermi function. Also based on approximate expression, the spectra suggested by ICRU[23] are reproduced for comparison in Figure 1.

Table 1. $Log-f$ values calculated for the allowed and first forbidden unique transitions.

Z	A	E_0^* (MeV)	spectral shapes					
			allowed			first forbidden		
			$Log-f_0^-$			$Log-f_1^-$		
			present work	Gove & Martin	Diff(%)	present work	Gove & Martin	Diff(%)
10	20	0.05	-3.755	-3.755	0.0	-4.964	-4.963	0.0
		0.5	-0.366	-0.366	0.0	-0.258	-0.257	-0.4
		5.0	3.776	3.776	0.0	5.588	5.588	0.0
30	70	0.05	-3.210	-3.21	0.0	-4.302	-4.30	0.0
		0.5	-0.000	-0.00	0.0	-0.085	-0.09	0.0
		5.0	4.020	4.02	0.0	5.828	5.83	0.0
50	120	0.05	-2.776	-2.776	0.0	-3.697	-3.694	-0.1
		0.5	0.389	0.389	0.0	0.451	0.452	-0.2
		5.0	4.303	4.304	0.0	6.101	6.102	-0.0
70	170	0.05	-2.346	-2.347	0.0	-3.140	-3.147	-0.2
		0.5	0.797	0.799	-0.3	0.840	0.844	-0.5
		5.0	4.599	4.600	0.0	6.557	6.559	0.0
80	200	0.05	-2.112	-2.112	0.0	-2.873	-2.888	-0.5
		0.5	1.022	1.024	-0.2	1.050	1.055	-0.5
		5.0	4.758	4.760	0.0	6.397	6.398	0.0
90	230	0.05	-1.859	-1.857	-0.1	-2.608	-2.637	-1.1
		0.5	1.265	1.269	-0.3	1.274	1.280	-0.5
		5.0	4.927	4.929	0.0	6.727	6.729	0.0

*maximum end-point energy. Note that $E_0 = m(W_0 - 1)$ where m is the rest mass energy of the electron.

Table 2. Nuclear data for the radionuclides considered.

nuclide	transition states		transition rate (%)	E_0 (MeV)	shape factor
	initial	final			
^{32}P	1^+	0^+	100.0	1.711	
^{90}Y	2^-	0^+	100.0	2.288	
^{131}I	$7/2^+$	$11/2^-$	0.43	0.812	
		$5/2^+$	89.0	0.608	
		$7/2^+$	7.67	0.335	
		$7/2^-$	0.6	0.305	
		$5/2^+$	2.17	0.250	
^{153}Sm	$3/2^+$	$5/2^+$	21.0	0.813	
		$5/2^-$	0.6	0.716	
		$3/2^+$	44.0	0.710	
		$7/2^-$	0.3	0.661	
		$5/2^+$	34.0	0.640	
^{166}Ho	0^-	0^+	52.0	1.857	$1 - 0.87\ W - 1/W + 0.22\ W^2 - 0.02\ W^3$
		2^+	47.0	1.776	
		0^+	0.7	0.428	
		1^-	0.2	0.215	
^{169}Er	$1/2^-$	$1/2^+$	55.0	0.340	
		$3/2^+$	45.0	0.330	
^{188}Re	1^-	0^+	70.0	2.116	$1 + 0.034\ (q^2 + p^2)$
		2^+	27.0	1.965	$1 + 0.038\ (q^2 + p^2)$
		2^+	1.7	1.483	
		0^+	0.7	1.030	
		2^-	0.6	0.654	
^{192}Ir	4^-	4^+	48.2	0.672	
		3^+	41.4	0.537	
		4^+	5.63	0.240	
		3^-	0.11	0.0782	
^{198}Au	2^-	2^+	98.6	0.961	$1 - 0.057\ W$
		2^+	1.3	0.285	

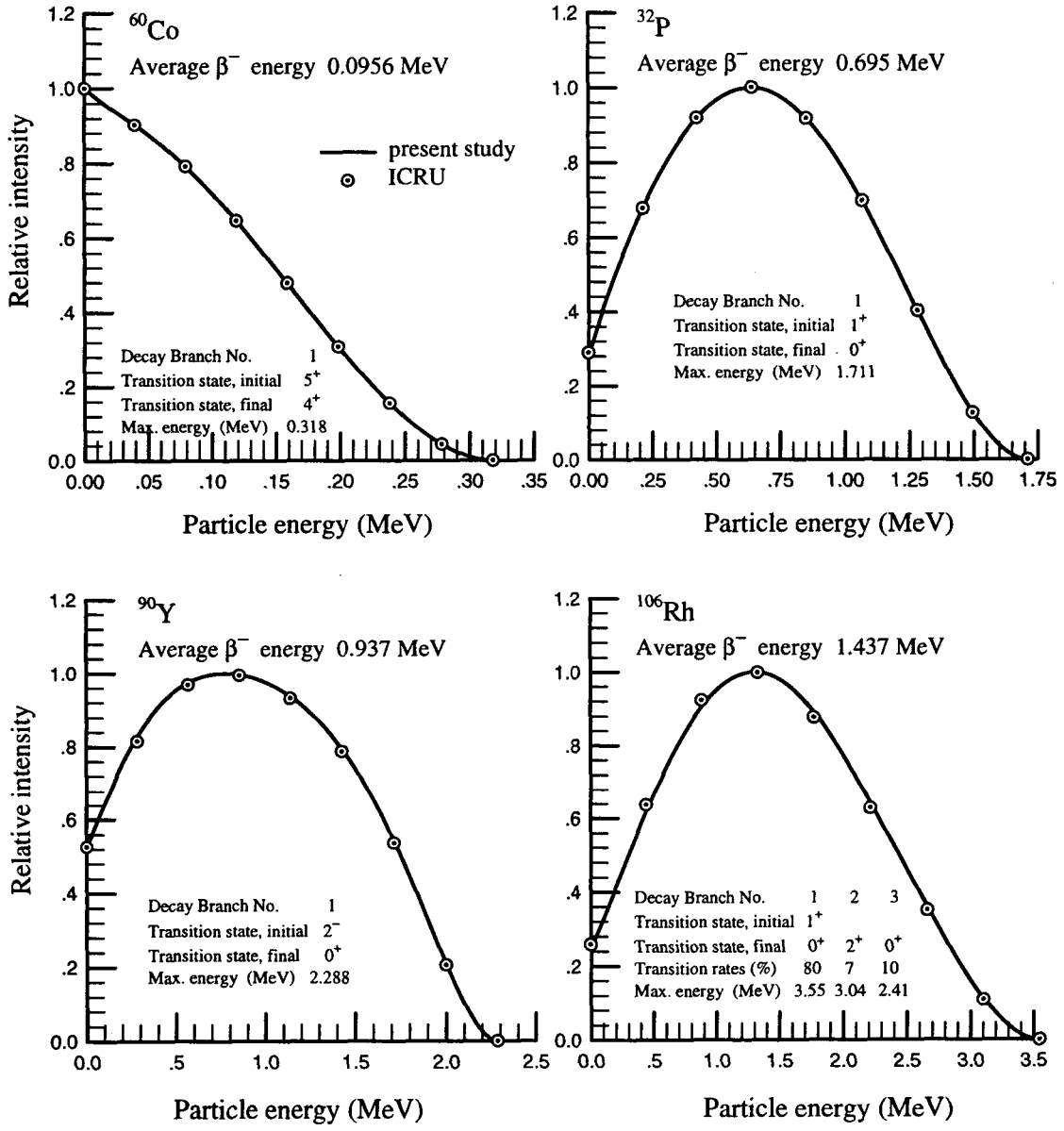

Fig. 1. Comparison of beta-spectra for the selected beta-emitters. In case of ^{60}Co, there exist two beta-decay branches: the one on the figure, and the other with decay rate of 0.12% and maximum end point energy of 1.48 MeV. For illustrative reason, the latter is ignored.

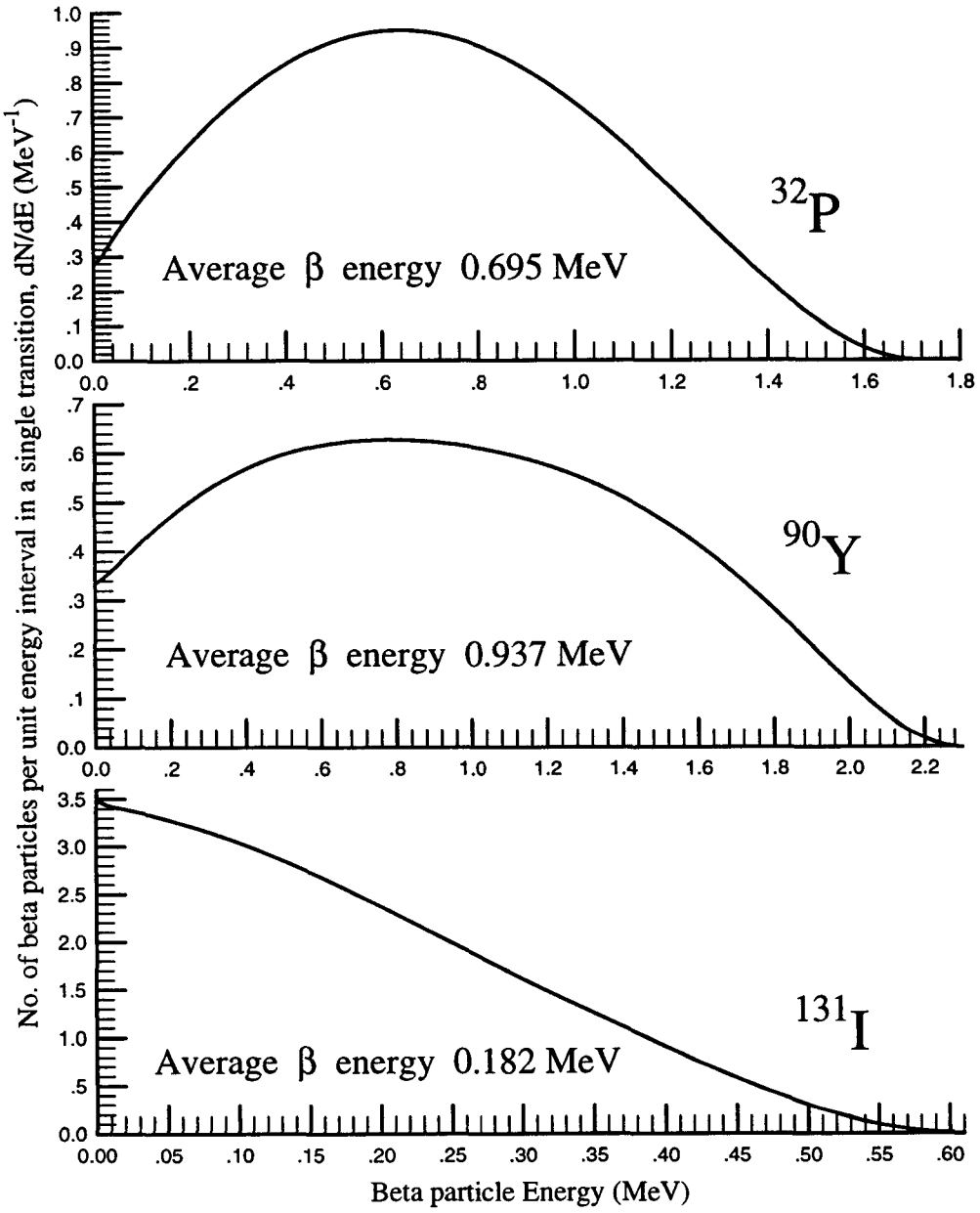

Fig. 2. Beta-spectra for the radionuclides in medicine. The area under a curve is normalized to the total number of beta-particles in a single transition, which is less than unity in case electron capture transitions go simultaneously.

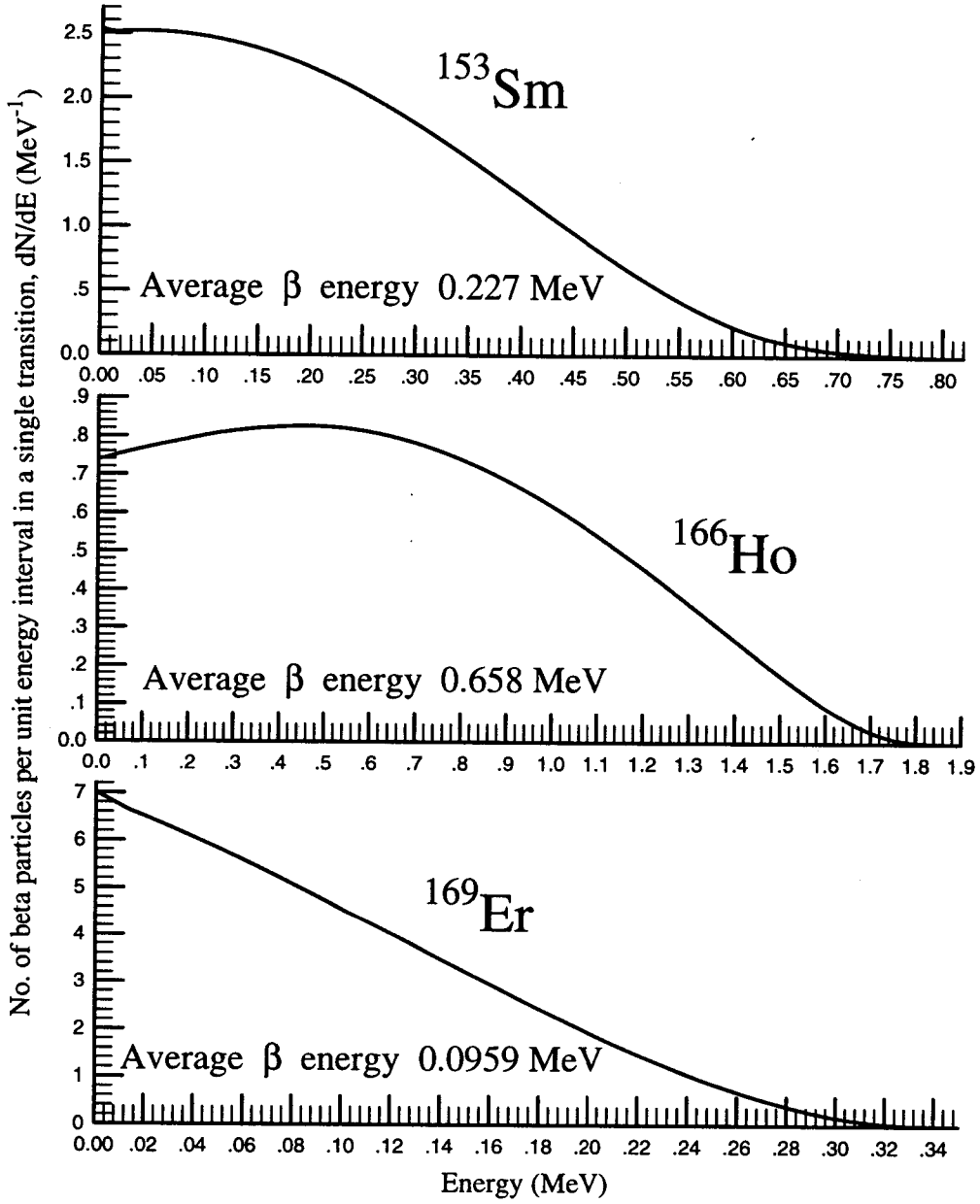

Fig. 2. (continued).

A total of 9 beta-spectra for ^{32}P, ^{90}Y, ^{131}I, ^{166}Ho, ^{192}Ir, ^{198}Au, ^{153}Sm, ^{169}Er and ^{188}Re are given in Figure 2 and Table 3. The area under the curve in Figure 2 is normalized to the total number of beta-particles in a single transition so that it can be less than unity when the transitions are induced simultaneously by an orbital electron capture.

Although the physics and mathematics on the electron and positron transport in medium have been well known for decades, beta-dosimetry continues to remain an uneasy problem since, as mentioned above, beta-dose profile is dependent of the spectral shapes of beta-ray energy distributions. When measurement of beta-spectra is made with the usual charged particle detectors, the uncertainty of the measured spectra is inevitably increased: the number of beta-particles in low energy region is reduced considerably and the spectrum is shifted toward lower energy because of the energy loss in windows materials and dead-layers. In general, the measured spectra is not appropriate for beta-dosimetry in medical applications, especially, formulation of beta-particle transport equation or Monte Carlo tracking of beta-particle trajectories. We calculated the beta-spectra using the exact expressions and shape factors. The hypergeometric and gamma functions were computed with an accuracy of better than 10^{-4}%. Consequently, the spectra presented are considered to be used in beta-dose evaluation with the least loss of accuracy.

CONCLUSION

It is necessary to maintain dose uniformity among medical institutions to provide safe and efficient radiation therapy. For obtaining beta-dose uniformity, accurate beta-particle energy distributions are prerequisite. In the present study, a total of 9 beta-spectra for ^{32}P, ^{90}Y, ^{131}I, ^{166}Ho, ^{192}Ir, ^{198}Au, ^{153}Sm, ^{169}Er and ^{188}Re are calculated with enough accuracy using the solutions of Dirac wave equation for a point-nucleus unscreened Coulomb potential. Corrections are made for the screening by the orbital-electrons and the finite size of the nucleus. It is expected that the calculated beta-spectra improve the accuracy of the beta-dose evaluation and accordingly, contribute to induce beta-dose uniformity.

REFERENCES

1. Cross WG, Wong PY and Freedman NO (1991) Dose distributions for electrons and beta rays incident normally on water. Radiat Prot Dosim 35: 77-91
2. Fano U (1952) Tables for the analysis of beta spectra. National Bureau of Standards Applied Mathematics Series 13 National Bureau of Standards
3. Dismuke N, Rose ME, Perry CL and Bell PR (1952) Fermi functions for allowed beta transitions. ORNL-1222, Oak Ridge National Laboratory
4. Rose ME, Perry CL and Dismuke NM (1953) Tables for the analysis of allowed and forbidden beta transition. ORNL-1459, Oak Ridge National Laboratory
5. Behrens H and Jänecke J (1969) Numerical data and functional relationships in science and technology. Landolt-Börnstein, Group I Nuclear physics and technology 4 Numerical tables for beta decay and electron capture Schopper H ed, Berlin Springer-Verlag
6. Marinelli LD, Brinckerhoff RF and Hine GJ (1949) Average energy of beta-rays emitted by radioactive isotopes. Rev Mod Phys 19:25-28
7. Paul H (1966) Shapes of beta spectra. Nucl Data 2:281-298.
8. Mantel J (1972) The beta ray spectrum and the average beta energy of several isotopes of interest in medicine and biology. Int J Appl Radiat Isotopes 23:407-413.
9. Cross WG, Ing H and Freedman N (1983) A short atlas of beta-ray spectra. Phys Med Biol 28(11):1251-1260.
10. Yi CY, Han HS, Cho WK, Park UJ, Jun JS and Chai HS (1998) Calculation of mass attenuation coefficients of beta particles. Radiat

Prot Dosim (in press: preprint is available on request to C. Y. Yi).
11. Gove NB and Martin MJ (1971) Log-f tables for beta decay. Nucl Data Tables 10:205-317.
12. Warburton EK, Harris WR and Alburger DE (1968) Beta decay of N^{16} to the 6.05 MeV state of O^{16}. Phys Rev 175:1275-1282.
13. Konopinski EJ (1966) *The theory of beta radioactivity*. Oxford Univ. Press, London, 179-202
14. Longmire C and Brown H (1949) Screening and relativistic effects on beta spectra. Phys Rev 75:264-270
15. Matese JJ and Johnson WR (1966) Screening corrections to the Fermi function for allowed β decay. Phys Rev 150(3):846-851.
16. Schopper HF (1966) Weak interactions and nuclear beta decay. North-Holland, Amsterdam 44
17. Lederer CM and Shirley VS (1978) *Table of isotopes*. 7-th edn New York Wiley.
18. Behrens H and Szybisz L (1976) Shapes of beta spectra. Phys Data 6-1
19. Wapstra AH (1958/1959) Shape factors for first forbidden non-unique beta transitions. Nucl Phys 9:519-527.
20. Bühring W (1963) Beta decay theory using exact electron radial wave functions. Nucl Phys 40:472-488.
21. Behrens H and Bühring W (1971) Nuclear beta decay. Nucl Phys A162:111-144.
22. Daniel H (1968) Shapes of beta-ray spectra. Rev. Mod Phys 40(3):659-672.
23. ICRU(International Commission on Radiation Units and Measurements) (1997) *Dosimetry of external beta rays for radiation protection*. report 56 Bethesda, MD, ICRU Publ